## **OPEN ACCESS**



## Detection of Young Massive White Dwarfs in Core-collapsed Globular Cluster NGC 362

R. K. S. Yadav<sup>1</sup>, Arvind K. Dattatrey<sup>1,2</sup>, Annapurni Subramaniam<sup>3</sup>, Geeta Rangwal<sup>1</sup>, and Ravi S. Singh<sup>2,4</sup>
Aryabhatta Research Institute of Observational Sciences, Manora Peak, Nainital 263002, India; rkant@aries.res.in, Physics.arvind97@gmail.com

Deen Dayal Upadhyay Gorakhpur University, Gorakhpur, Uttar Pradesh 273009, India

Indian Institute of Astrophysics, Koramangala, Bangalore 560034, India

Maa Pateshwari University, Balarampur, Uttar Pradesh 271201, India

Received 2025 May 2; revised 2025 July 29; accepted 2025 August 6; published 2025 September 9

#### Abstract

Core-collapsed globular clusters are ideal targets to explore the presence of stellar collision products. Here, we have studied 17 far-UV bright white dwarf (WD) members in the globular cluster NGC 362 using data obtained from the Ultra Violet Imaging Telescope (UVIT) mounted on AstroSat and from the Hubble Space Telescope. Multiwavelength spectral energy distributions (SEDs) are analyzed using UV and optical data sets to characterize and determine the parameters of WDs. Fourteen of the WDs fit single-component SEDs well, while three showed a good fit with a two-component SED model, indicating a binary system comprising a WD and a low-mass main-sequence (MS) star. The effective temperatures, radii, luminosities, and masses of WDs are in the ranges 22,000–70,000 K, 0.008–0.028  $R_{\odot}$ , 0.09–3.0  $L_{\odot}$ , and 0.30–1.13  $M_{\odot}$ , respectively. The effective temperatures, radii, luminosities, and masses of the companions (low-mass MS stars) are 3500–3750 K, 0.150–0.234  $R_{\odot}$ , 0.003–0.01  $L_{\odot}$ , and 0.14–0.24  $M_{\odot}$ , respectively. The three binary systems (WD-MS), along with the massive WDs, may have formed through dynamical processes that occurred during the core collapse of the cluster. This is the first evidence of a massive WD formation in a core-collapsed cluster, which is the missing link in the formation of a fast radio burst (FRB) progenitor in a globular cluster. This study provides evidence that NGC 362 hosts stellar systems that may evolve into exotic stars such as Type Ia supernovae and/or FRBs in the future. This Letter is paper VI of the Globular Cluster UVIT Legacy Survey.

Unified Astronomy Thesaurus concepts: White dwarf stars (1799); M dwarf stars (982)

## 1. Introduction

White dwarfs (WDs) are the remains of low-to-intermediate-mass main-sequence (MS) stars (L. G. Althaus 2010; F. M. Jimenez-Esteban et al. 2023). Globular clusters are expected to contain tens of thousands of WDs. However, the observational study of these WDs has been slow due to their low luminosity (H. B. Richer 1978; R. A. W. Elson et al. 1995). In the mid-1990s, significant progress was made with the observation of large WD populations and the WD cooling sequence in various globular clusters (H. B. Richer et al. 1995, 1997; A. M. Cool et al. 1996; A. Renzini et al. 1996; B. M. S. Hansen et al. 2007; A. Calamida et al. 2008).

Additionally, the study of WD-MS systems is an important research area because they constitute a common final-stage object of stellar evolution, a WD, and the most frequent type of star, the M spectral type component. Close WD-MS binaries are also progenitor candidates for cataclysmic variables and Type Ia supernovae (T. P. G. Wijnen et al. 2015; D. Liu et al. 2019).

The *N*-body simulations of globular clusters have shown that massive WDs can be found in the central regions of corecollapsed globular clusters (K. Kremer et al. 2020; N. Z. Rui et al. 2021). Recent studies show that NGC 6397 harbors a massive central region with the possibility of hosting a few stellar black holes at present day (N. C. Weatherford et al. 2020; N. Z. Rui et al. 2021; E. Vitral et al. 2022). R. R. Strickler et al. (2009) found that some of the He WDs might be binaries with

Original content from this work may be used under the terms of the Creative Commons Attribution 4.0 licence. Any further distribution of this work must maintain attribution to the author(s) and the title of the work, journal citation and DOI.

massive dark CO WD companions. M. Pichardo Marcano et al. (2025) detected WDs in the mass range 0.18  $M_{\odot} \leqslant M \leqslant 0.5~M_{\odot}$  and a second candidate for a magnetic He core WD. NGC 6397 is, therefore, a core-collapsed globular cluster (S. C. Trager et al. 1995) that harbors exotic systems, and K. Kremer et al. (2021) used this cluster to simulate WD systems in such systems.

The recent discovery of a fast radio burst (FRB) repeater in an old globular cluster in M81 (F. Kirsten et al. 2022) has prompted the astronomical community to investigate potential progenitors. The magnetar model has emerged as the most accepted model for FRBs (E. Petroff et al. 2019). There have been studies to explore and identify probable progenitor populations for an FRB in a globular cluster (K. Kremer et al. 2023b). A massive WD binary merger, as suggested by K. Kremer et al. (2021), may provide a natural formation mechanism for this repeater.

Recently, A. K. Dattatrey et al. (2023a) detected WD-MS binaries, apart from the detection of WD companions to blue stragglers in NGC 362 (A. K. Dattatrey et al. 2023b). They attributed many binary systems to the recent core collapse of the cluster (A. K. Dattatrey et al. 2023a, 2023b). As this is a core-collapsed cluster, it is important to check its WD population. This study aims to detect and analyze the WD systems in the globular cluster NGC 362 to determine their fundamental parameters and nature.

The Letter starts with an introduction in Section 1, followed by a description of observations and methodology in Sections 2 and 3. Section 4 provides details about the spectral energy distributions (SEDs) and the parameters of the WDs, with the H-R diagram of WDs and their companions in

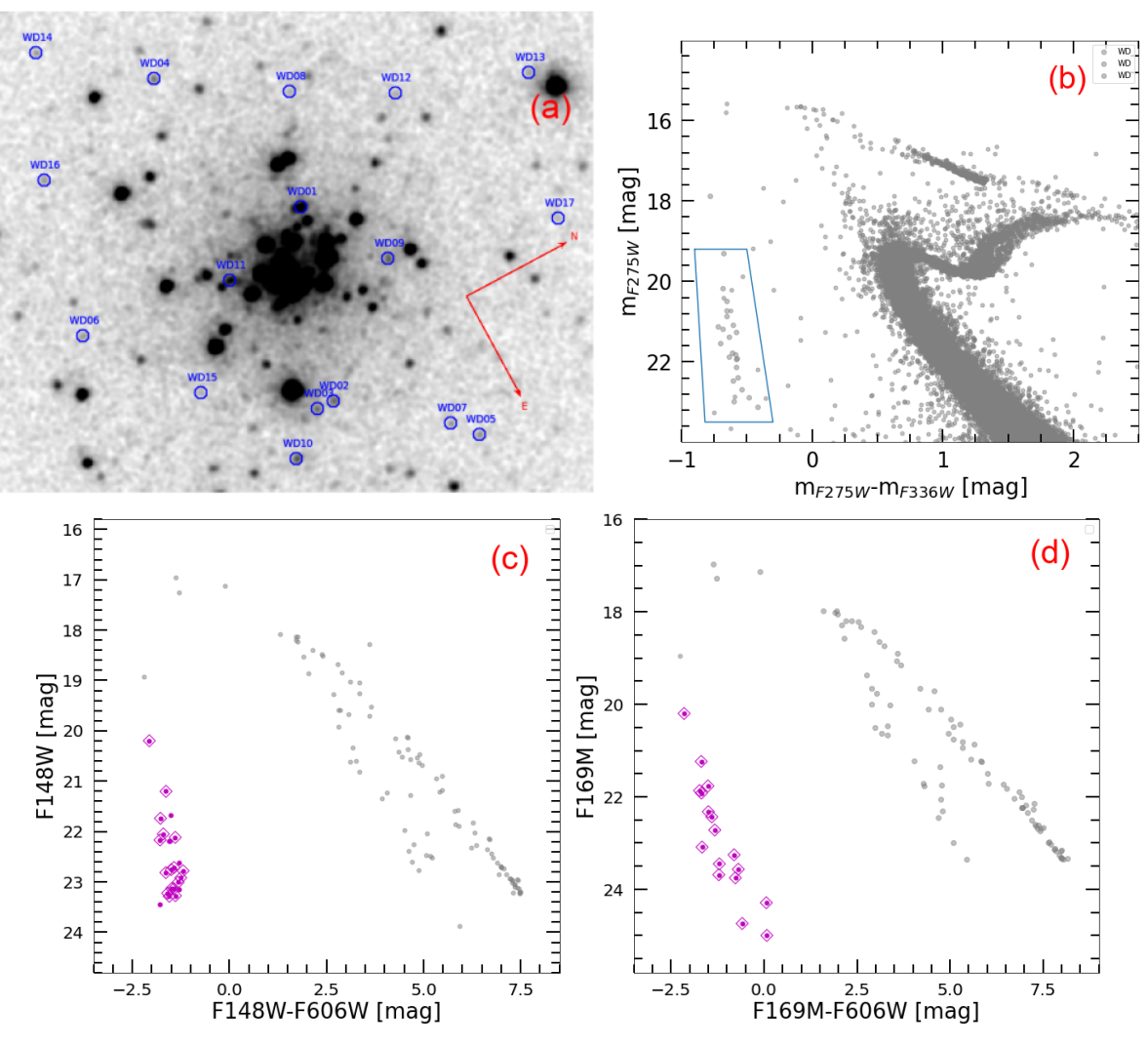


**Figure 1.** (a) The FUV image of  $1.75' \times 1.75'$  for the cluster NGC 362 in the F148 filter. Directions are shown in the figure. The 17 FUV bright WDs are shown with the star ID numbers. Panel (b) shows the  $(m_{\rm F275W}-m_{\rm F336W})$  vs.  $m_{\rm F275W}$ , while panels (c) and (d) show the (F148W-F606W) vs. F148W and (F169M-F606W) vs. F169M CMDs. Magenta color in panels (c) and (d) represents the WDs. The open magenta squares represent the WDs without contamination from neighboring stars.

Section 5, followed by discussions in Section 6. A summary and conclusions of our work are given in the final section.

## 2. Observations

The observational data for the globular cluster NGC 362 in UV were collected using the Ultra Violet Imaging Telescope (UVIT) mounted on AstroSat, India's first multiwavelength space observatory. The observations took place on 2016 November 11, using two UV filters: F148W and F169M. The exposure times for the filters were 4900 and 4600 s, respectively. The identification map for the cluster in filter F148 is depicted in Figure 1(a). The raw images were processed using CCDLAB software (J. E. Postma & D. Leahy 2017), which corrects for satellite drift, flat-field, geometric distortion, fixed pattern noise, and cosmic rays. Detailed descriptions of the telescope, instruments, and preliminary calibration can be found in A. Subramaniam et al. (2016) and S. N. Tandon et al. (2017). The photometry was done using the DAOPHOT routine developed by P. B. Stetson (1987). We conducted point-spread function (PSF) photometry, a technique particularly useful for analyzing crowded regions. To determine the PSF, we used several well-isolated brighter stars. By analyzing the light

distribution of isolated stars, we generated a model of the PSF for a given image. The PSF model is then fitted to each detected star in the image. Once the PSF is fitted, it is subtracted from the star's image, effectively removing the contribution of that star's light from the surrounding pixels. As a result, we obtained PSF magnitudes for all the stars in the image. The photometric depth in the F148 band is  $\sim$ 23.0 mag.

## 3. Selection of White Dwarfs

We used the near-UV-far-UV (FUV) and FUV-optical color-magnitude diagrams (CMDs) to select the WDs for the present analysis. We compared our UVIT catalog with the Hubble Space Telescope (HST) UV HUGS catalog (D. Nardiello et al. 2018) to find the optical counterparts of WDs. The HUGS catalog provides the HST magnitudes in F275, F336, F438, F606, and F814 filters. In Figure 1(b), we have plotted the HST CMD in the ( $m_{\rm F275W}$ - $m_{\rm F336W}$ ),  $m_{\rm F275W}$  plane. This diagram shows a hot stellar population, including horizontal branch (HB) stars, blue stragglers, and WDs. There is a vertical sequence ranging from  $\sim$ 19 to 23 in  $m_{\rm F275W}$  mag and with a color of approximately -0.65 mag in ( $m_{\rm F275W}$ - $m_{\rm F336W}$ ), representing the WD sequence. A blue trapezoidal box depicts

the boundary of the WD sequence. In this way, we identified 33 WDs in the blue rectangle box.

In Figures 1(c) and (d), we present the FUV-optical CMD ((F148-F606) versus F148 and (F169M-F606) versus F169M) of the hot population of the cluster. We found 23 FUV bright WDs common in the HST and UVIT catalog and shown with magenta points. Furthermore, we checked the contamination in flux from nearby stars of these WDs by comparing the aperture magnitudes with the PSF magnitudes. The PSF photometry reduces contamination by  $\sim 3\%$  if any contamination is present. Finally, we found 17 noncontaminated WDs having UV and optical data and marked them in Figure 1(a) with their IDs. All 17 WDs are members of the cluster based on the analysis by M. Soto et al. (2017). We considered these WDs for further study.

## 4. Spectral Energy Distribution of White Dwarfs

In this section, we build the SED for 17 WDs to analyze their basic parameters and characteristics using the virtual observatory tool VO SED Analyzer (VOSA; A. Bayo et al. 2008). The reddening E(B-V) = 0.05 mag from W. E. Harris (2010) and distance of 8.83 Kpc are taken from E. Vasiliev & H. Baumgardt (2021). VOSA utilizes filter transmission curves to calculate synthetic photometry based on a selected theoretical model. The synthetic photometric data are then compared to the observed data, and the best fit is determined using the  $\chi_r^2$  minimization test, as explained in A. K. Dattatrey et al. (2023b). In summary, we fitted the D. Koester (2010) model, considering variations in temperature and log g. The effective temperatures ranged from 5000 to 80,000 K, with log g ranging from 5 to 9.5 dex. The SED was generated using photometric data covering UV to optical wavelengths. Initially, we fitted a SED with a single component, as shown by the gray curve in Figure 2. The data points used for fitting are represented by cyan and red-filled circles with error bars, while model data points are shown in blue. The difference between the fitted model and the observed fluxes, normalized by the observed flux, is displayed in the lower panel of Figure 2. The dashed horizontal lines at  $\pm 0.3$  (30%) represent the threshold. Except for WD 15, WD 16, and WD 17, the residual plot for all the WDs is within  $\pm 0.3$ . This suggests that a single SED fits all WDs except WD 15, WD 16, and WD 17. The derived parameters and the fitting parameters for the single-component WDs are listed in Table 1.

The residual plot for WD 15, WD 16, and WD 17 reveals that the near-IR residual flux is more significant than 0.3, as shown with the red points in the bottom panels of Figure 2. The residuals indicate that a single-component SED does not fit well in the near-IR region. The fitting shows a near-IR excess in the SEDs. Therefore, a combination of hot and cool spectra is tried. A two-component SED is fitted for WD 15, WD 16, and WD 17, as depicted in Figure 2. The gray curve represents the D. Koester (2010) model corresponding to the hot component, while the F. Castelli & R. L. Kurucz (2003) model shown in the sky-blue curve represents the cool component. The combined spectrum is shown with a black curve. The residual plot represented with blue points shows that the combined spectrum fits well. The fitting parameters, along with the characteristic parameters, are listed in Table 1.

The fundamental parameters of the 17 WDs derived using SED fit are listed in Table 1. For WDs, the fundamental parameters are in the range of  $T_{\rm eff}\sim 22{,}000{-}70{,}000\,$  K, log  $g\sim 6.5{-}9.5,$ 

 $L\sim0.09-3.0~L_{\odot}$ , and  $R\sim0.008-0.028~R_{\odot}$ . The parameters of the cool companions of WD 15, WD 16, and WD 17 are in the range  $T_{\rm eff}\sim3500-3750~$  K, log g=0.5-3.0, [Fe/H]  $\sim-1.0$ ,  $L\sim0.003-0.010~L_{\odot}$ , and  $R\sim0.150-0.234~R_{\odot}$ . The goodness-of-fit parameters, i.e.,  $\chi^2_r$ ,  $V_{gf}$ , and  $V_{gfb}$ , are also listed in Table 1. The  $V_{gf}$  and  $V_{gfb}$  are the modified reduced  $\chi^2_r$  provided by VOSA by assuming the observational errors of 2% and 10% of the observed flux, respectively. These parameters provide a visual check of the fit quality, with recommended thresholds of  $V_{gf}\!\!\!<25$  or  $V_{gfb}\!\!<15$  (F. M. Jiménez-Esteban et al. 2018; A. Rebassa-Mansergas et al. 2021).

# 5. H-R Diagram of the White Dwarfs and Their Companions

After obtaining the essential parameters of WDs, we created the HR diagram in Figure 3. The WDs are shown with magenta points, while the blue points represent the cool companions of WD 15, WD 16, and WD 17. The theoretical isochrone (S. L. Hidalgo et al. 2018; A. Pietrinferni et al. 2021) is plotted with the black line using the fundamental parameters of the cluster taken from W. E. Harris (2010). We superimposed WD cooling curves taken from P. E. Tremblay & P. Bergeron (2009) for various masses, distinguished by colors. Our analysis utilized the pure hydrogen (DA) models of WDs. We are unable to clearly distinguish between DA and pure helium (DB) WDs based on the current analysis. This limitation in differentiating between the two types of WDs has led us to apply a DA model for our analysis. To determine the mass of the WDs, we performed interpolation using their cooling curves. We generated 10 submodels based on theoretical cooling curves, each within a mass interval of  $0.1 M_{\odot}$ , to improve the accuracy of our mass estimates. In this way, we estimated the WD masses from 0.30 to 1.13  $M_{\odot}$ , with a cooling age ranging from 0.2 to 35 million years. We also assessed the mass and age of the WDs using DB models, and the results were consistent within the margin of error. We note that the WDs were formed very recently and have a large mass range.

Mass of the cool companions. The cool companions (WD 15B, WD 16B, WD 17B) follow the isochrone of 11 Gyr and are located in the lower part of the main sequence. We estimated the mass of cool companions in the range  $0.14-0.24~M_{\odot}$ . Based on the location in the H-R diagram and parameters derived in the previous section for the cool companions, we may conclude that they may be M-type dwarf stars on the MS.

Low-mass WDs. The minimum mass of WDs formed through single-star evolution is 0.4  $M_{\odot}$  (W. R. Brown et al. 2010). Out of the 17 WDs studied, three (WD 04, WD 05, and WD 14) fall within the mass range of 0.3–0.4  $M_{\odot}$ . According to M. Kilic et al. (2007), the low-mass helium-core WDs  $(M < 0.45 M_{\odot})$  can be produced from interacting binary systems, and generally, all of them have been attributed to this channel. However, these WDs may also arise from a single star that experiences significant mass loss during the red giant branch phase. Single low-mass WDs are detected in many studies. A Palomar-Green (PG) survey done by J. Liebert et al. (2005) found 30 low-mass WDs. About 47% of the low-mass WDs in the PG survey that were searched for companions seemed to be single (M. Kilic et al. 2007). The ESO SN Ia Progenitor Survey searched for radial velocity variations in more than a thousand WDs using the Very Large Telescope

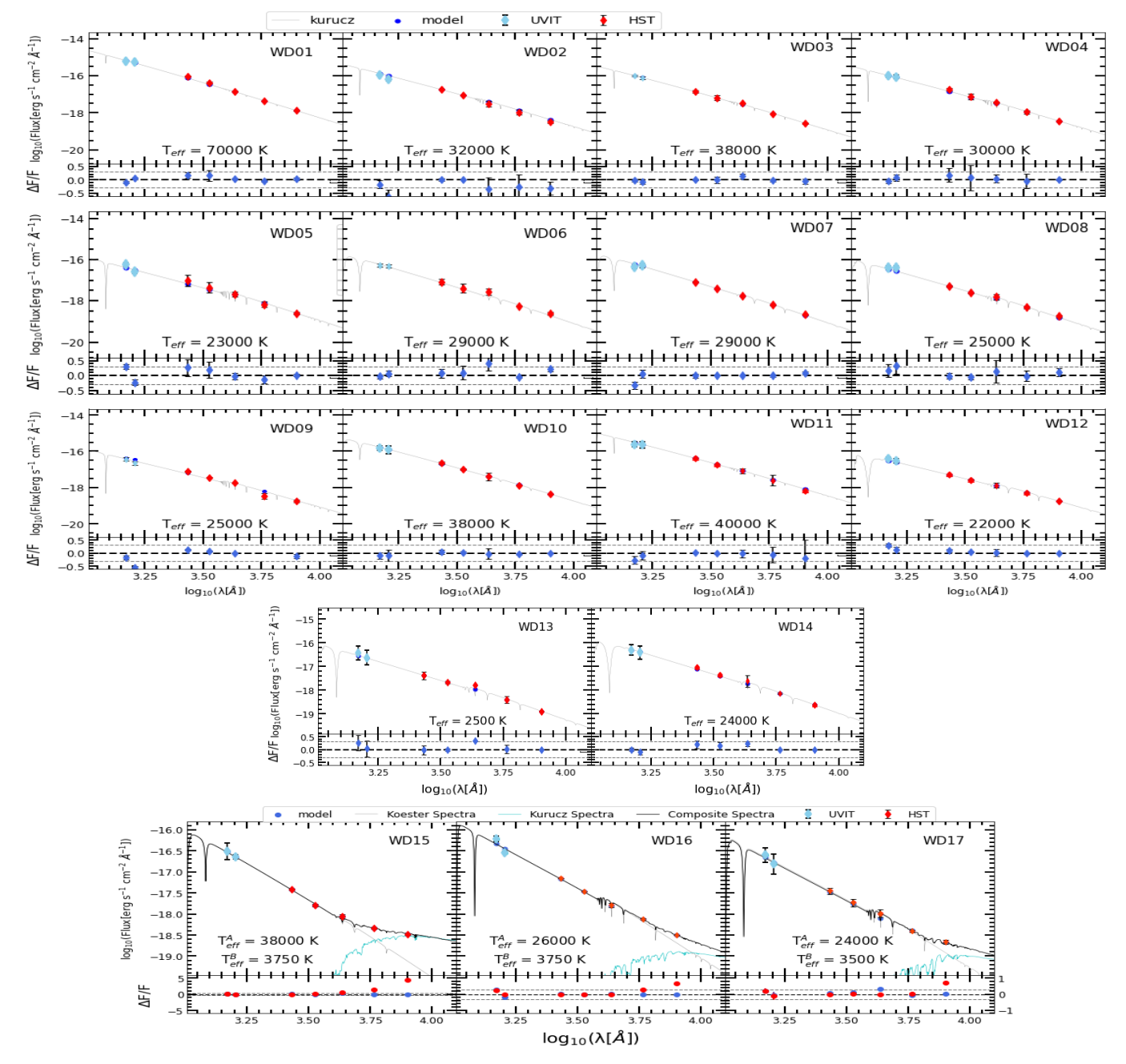


Figure 2. The SEDs of the 14 single-component and three two-component (WD 15, WD 16, and WD 17) WDs. The blue points represent the synthetic flux from the model used to fit the observed SED. The  $T_{\rm eff}$  values of the hot (A) and cool (B) components are displayed for the two-component WDs. The UVIT and HST data points are represented in cyan and red, while the model data are represented with blue points. The D. Koester (2010), F. Castelli & R. L. Kurucz (2003), and combined spectra are shown by gray, cyan, and black curves, respectively.  $\Delta F/F$  is the fractional residual.

(R. Napiwotzki & Eso Sn Ia Progenitor Search Consortium 2001). They found that 15 of these low-mass WDs do not show any radial velocity variations, corresponding to a single low-mass WD (R. Napiwotzki et al. 2007).

Normal and slightly massive WDs. Additionally, 12 WDs (WD 02, WD 03, WD 06, WD 07, WD 08, WD 09, WD 10, WD 11, WD 12, WD 13, WD 16, and WD 17) fall within the mass range of 0.4–0.6  $M_{\odot}$ . Among these, WD 16 and WD 17 are binary systems, with WD masses of 0.39  $M_{\odot}$  and 0.48  $M_{\odot}$  and companion masses of 0.16  $M_{\odot}$  and 0.14  $M_{\odot}$ , respectively. The WDs having a mass between 0.4 and 0.6  $M_{\odot}$  are likely to have formed via single-star evolution. In globular clusters, WDs are currently produced by progenitors with stellar masses

of about  $0.8-1.0~M_{\odot}$  (S. Moehler & G. Bono 2011). The cooling age of these WDs is  $0.2-15~\rm Myr$ , indicating that they have formed quite recently. As the progenitor mass is slightly more than the turn-off mass, some of the progenitor stars may be blue stragglers, which could have formed as a result of stellar mergers or mass transfer between stars in binary systems. Over time, blue stragglers evolve and, eventually, end their lives as WDs (F. R. Ferraro et al. 2009; S. Moehler & G. Bono 2011). A. K. Dattatrey et al. (2023b) detected extremely low-mass WD companions to 12 blue stragglers in this cluster. They also found that the blue stragglers of this cluster may have a mass up to  $1.64~M_{\odot}$ . The massive blue stragglers are likely to be the progenitors of WDs with masses

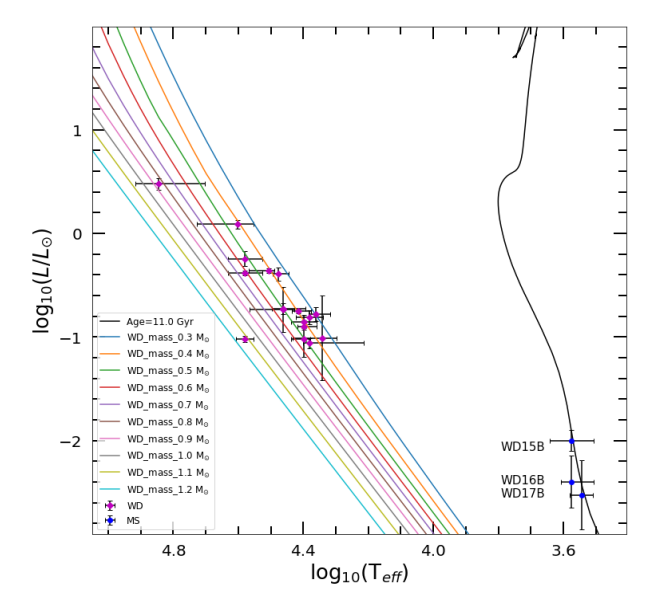
Yadav & Dattatrey et al.

 Table 1

 The Best-fit Parameters for the WDs and their Companions

Name	R.A.	Decl.	r	T <sub>eff</sub> (K)	log g	$L/L_{\odot}$	$R/R_{\odot}$	$\chi_r^2$	$V_{ m gf}$	$V_{ m gfb}$	$N_{ m fit}/N_{ m tot}$	$M/M_{\odot}$	Age (Myr)
WD 01	15.79445	-70.84506	20.3	$70000^{+5000}_{-10000}$	6.5	$2.997^{+0.160}_{-0.180}$	$0.028^{+0.002}_{-0.003}$	31.48	5.82	1.15	7/7	$0.86^{+0.08}_{-0.16}$	0.7
WD 02	15.84468	-70.85072	40.0	$32000^{+2000}_{-500}$	6.5	$0.434^{+0.010}_{-0.020}$	$0.022^{+0.001}_{-0.002}$	43.12	8.62	4.33	7/7	$0.41^{+0.12}_{-0.04}$	0.6
WD 03	15.84460	-70.85229	45.3	$38000^{+2000}_{-2000}$	6.5	$0.415^{+0.010}_{-0.020}$	$0.017^{+0.001}_{-0.001}$	36.83	0.74	0.49	7/7	$0.62^{+0.07}_{-0.06}$	1.5
WD 04	15.74530	-70.85113	75.4	$30000^{+500}_{-1000}$	6.5	$0.405^{+0.026}_{-0.040}$	$0.024^{+0.001}_{-0.001}$	2.97	0.59	0.44	7/7	$0.35^{+0.02}_{-0.03}$	0.6
WD 05	15.87124	-70.84074	79.0	$23000^{+500}_{-1000}$	6.5	$0.166^{+0.011}_{-0.019}$	$0.025^{+0.001}_{-0.001}$	23.17	4.63	3.43	7/7	$0.30^{+0.02}_{-0.10}$	2.2
WD 06	15.79724	-70.86747	69.4	$29000^{+3000}_{-1000}$	9.5	$0.185^{+0.040}_{-0.010}$	$0.017^{+0.001}_{-0.002}$	25.84	5.17	2.90	7/7	$0.50^{+0.14}_{-0.03}$	8.0
WD 07	15.86496	-70.84249	72.2	$29000^{+1000}_{-2000}$	9.5	$0.187^{+0.010}_{-0.010}$	$0.018^{+0.002}_{-0.001}$	23.19	4.46	2.32	7/7	$0.50^{+0.04}_{-0.06}$	8.0
WD 08	15.76577	-70.84111	56.8	$25000^{+500}_{-1000}$	8.5	$0.125^{+0.001}_{-0.010}$	$0.018^{+0.001}_{-0.001}$	31.92	6.38	3.18	7/7	$0.43^{+0.02}_{-0.04}$	10
WD 09	15.79257	-70.85373	26.0	$25000^{+1000}_{-1000}$	6.5	$0.139_{-0.010}^{+0.010}$	$0.020^{+0.001}_{-0.002}$	58.59	11.7	7.69	7/7	$0.41^{+0.04}_{-0.04}$	5.0
WD 10	15.854263	-70.856049	61.3	$38000^{+2000}_{-2000}$	9.5	$0.567^{+0.040}_{-0.020}$	$0.021^{+0.007}_{-0.005}$	31.06	3.2	0.436	7/7	$0.54^{+0.05}_{-0.05}$	3.5
WD 11	15.80346	-70.853723	19.4	$40000^{+5000}_{-2000}$	6.5	$1.222^{+0.050}_{-0.060}$	$0.028^{+0.006}_{-0.005}$	71.20	7.98	1.92	7/7	$0.41^{+0.10}_{-0.03}$	0.2
WD 12	15.78068	-70.833015	65.2	$22000^{+2000}_{-1000}$	9.5	$0.098^{+0.04}_{-0.003}$	$0.020^{+0.010}_{-0.008}$	46.83	5.1	2.11	7/7	$0.35^{+0.07}_{-0.03}$	7.0
WD 13	15.792786	-70.821661	97.5	$25000^{+1000}_{-500}$	8.5	$0.096^{+0.017}_{-0.003}$	$0.016^{+0.010}_{-0.004}$	07.07	1.76	1.65	6/7	$0.50^{+0.05}_{-0.02}$	15
WD 14	15.724402	-70.859252	105.2	$24000^{+1000}_{-1000}$	9.5	$0.155^{+0.010}_{-0.010}$	$0.022^{+0.010}_{-0.007}$	08.65	2.88	1.99	6/7	$0.35^{+0.04}_{-0.03}$	7.7
WD 15A	15.82578	-70.86067	49.0	$38000^{+1000}_{-1000}$	9.5	$0.096^{+0.005}_{-0.001}$	$0.008^{+0.001}_{-0.002}$	67.35	35.5	12.2	7/7	$1.13^{+0.02}_{-0.02}$	35
WD 15B				$3750^{+250}_{-250}$	0.5	$0.010^{+0.001}_{-0.001}$	$0.234^{+0.016}_{-0.032}$					$0.24^{+0.01}_{-0.01}$	
WD 16A	15.755527	-70.863951	83.2	$26000^{+500}_{-1000}$	7.0	$0.177^{+0.003}_{-0.016}$	$0.0202^{+0.007}_{-0.001}$	71.69	32.3	4.67	7/7	$0.39^{+0.02}_{-0.03}$	5.2
WD 16B				$3750^{+125}_{-250}$	3.0	$0.004^{+0.001}_{-0.0007}$	$0.1503^{+0.001}_{-0.001}$					$0.16^{+0.01}_{-0.01}$	
WD 17A	15.830937	-70.825606	86.2	$24000^{+500}_{-4000}$	7.5	$0.087^{+0.004}_{-0.005}$	$0.0162^{+0.007}_{-0.001}$	8.480	8.48	7.75	7/7	$0.48^{+0.03}_{-0.14}$	15
WD 17B				$3500^{+125}_{-125}$	3.0	$0.003^{+0.001}_{-0.002}$	$0.154^{+0.010}_{-0.010}$					$0.14^{+0.01}_{-0.01}$	

Note. The positions (R.A. and decl.) are provided in degrees, and r (in arcsec) denotes the distance from the cluster center. The  $T_{\rm eff}$  is the effective temperature in K,  $\log g$  is the surface gravity in the logarithm unit, and the reduced chi-square ( $\chi^2_r$ ), luminosity (L), and radius (R) are in solar units, while  $V_{gf}$  and  $V_{gfb}$  are the visual goodness of fit. The  $N_{\rm fit}$  is the number of points considered in the fitting, and  $N_{\rm tot}$  is the total number of points. M is the mass of the stars in solar units.



**Figure 3.** The H-R diagram of hot and cool components of the WDs. The red points represent the WDs, while the blue points represent the cool components (MS stars). The WD cooling curves for different masses are shown in different colors (defined in the legend). The black curve represents the isochrone taken from S. L. Hidalgo et al. (2018) and A. Pietrinferni et al. (2021).

between 0.5 and 0.6  $M_{\odot}$ . We therefore note that this cluster contains both blue stragglers and their progeny.

WD-MS binaries. In this analysis, we identified three binary systems (WD 15, WD 16, and WD 17) composed of WD and MS stars. These systems may not be primordial binaries, as primordial binaries can be disrupted by dynamic processes within the cluster (N. Ivanova et al. 2006). A simulation conducted by K. Kremer et al. (2021) showed that 65% of WD-MS binaries form through dynamical interactions rather than as primordial binaries. A. K. Dattatrey et al. (2023a) found four WD-MS systems, where the MS stars were found to have lowmass or extremely low-mass WD companions. The above systems are likely to be mass-transfer products, whereas the WD-MS systems detected in this study may or may not have undergone mass transfer. Indeed, a binary consisting of an MS star and a WD can form through several types of dynamical encounters: exchange interaction, tidal capture of an MS star by a WD, or physical collisions between a red giant and an MS star (N. Ivanova et al. 2006). Additionally, K. Kremer et al. (2021) demonstrated that WD-MS binaries can also form through dynamical interactions in the core-collapse globular clusters. Based on their cooling ages, we infer that these systems may have formed during the core-collapse phase of the cluster through dynamic processes. The typical mass of a WD capable of capturing an MS star is  $\sim 1.0 \pm 0.2 M_{\odot}$  (N. Ivanova et al. 2006). Numerical simulation conducted by N. Soker et al. (1987) indicates that within the core of a globular cluster, a  $0.8 M_{\odot}$  WD can collide with MS stars of masses between 0.2 and 0.4  $M_{\odot}$ . One of the WD-MS systems (WD 15) has an ultramassive WD (1.13  $M_{\odot}$ ) that may have formed via the collision of a WD binary, and it capturing an MS star of mass  $0.24 M_{\odot}$  is therefore possible. A fraction of these stars can become bound to the WD, while the remainder will be dispersed. A portion of these dynamically formed WD-MS binary systems will initiate mass transfer and evolve into cataclysmic variables.

Massive WDs. The mass distribution of WDs shows a main peak at  $\sim$ 0.6  $M_{\odot}$  and a smaller peak at the tail of the distribution

 $\sim$ 0.8  $M_{\odot}$  (S. J. Kleinman et al. 2013). The presence of massive WDs ( $M \geqslant 0.8~M_{\odot}$ ) and ultramassive WDs ( $M \geqslant 1.10~M_{\odot}$ ) has been discussed in several studies (J. J. Hermes et al. 2013; S. O. Kepler et al. 2016; B. Curd et al. 2017). In the present study, two WDs, WD 01 and WD 15, have masses greater than 0.8  $M_{\odot}$ . WD 01 is classified as a massive WD, while WD 15 is categorized as an ultramassive WD.

Based on velocity dispersion analysis, S. Cheng et al. (2020) concluded that about 20% of the single WDs with masses greater than 0.8  $M_{\odot}$  form through the merger of two WDs. In another study, K. D. Temmink et al. (2020) estimated, based on binary population synthesis studies, that from 30% to 45% of all the single WDs with masses larger than 0.9  $M_{\odot}$  are likely formed through binary mergers, and most of them via double WD mergers. Therefore, we expect that WD 01 and WD 15 may have formed due to the merger of binary WDs.

J. Chen et al. (2021) have studied the brightest portion of the WD cooling sequence in two twin, old, and massive globular clusters, M3 and M13. They found that the bright WDs in M13 may result from the cooling processes slowing down due to stable thermonuclear burning in the remaining hydrogen-rich envelope. Additionally, they concluded that this phenomenon occurs in M13 but not in M3, which is consistent with the different HB morphologies of the two clusters. The HB morphology of cluster NGC 362 resembles that of cluster M3, where such WDs are absent. Therefore, based on the HB morphology, we would not expect to find slow-cooling bright WDs in NGC 362.

## 6. Discussion

According to E. Dalessandro et al. (2013) and M. Libralato et al. (2018), NGC 362 is a post-core-collapse cluster, as indicated by its radial density profile and internal velocity dispersion. This cluster, therefore, is likely to show the signatures of core collapse and is an ideal target to look for massive WDs. The WDs analyzed in this study have a range in mass and are very young (cooling age ≤35 million years), suggesting that they have formed recently. Based on the cooling age, we infer that the massive WD (WD 01) and the ultramassive WD (WD 15) may have formed during the corecollapse phase. During this phase, it is possible that binary WDs merged, resulting in the formation of massive WDs (K. D. Temmink et al. 2020; K. Kremer et al. 2021). A slow  $(\sim 100 \text{ ms})$  radio pulsar was discovered in the globular cluster NGC 362 as part of the MeerKAT TRAPUM project.<sup>5</sup> K. Kremer et al. (2023a) have suggested that slow pulsars in globular clusters may form relatively recently through the merging of WDs. If this radio pulsar is indeed young, as has not yet been proven, we can expect that WD mergers are currently occurring in this cluster. K. Kremer et al. (2021) studied WD systems in core-collapsed globular clusters and predicted the existence of young massive WDs that are similar to WD 01 and WD 15. We suggest that NGC 362 is a potential target to study core-collapse dynamics resulting in the formation of massive compact objects.

The massive WDs, WD 01 and WD 15, are located at distances of 20" and 49" from the center of the cluster. While they are outside the core radius of 11", they fall within the half-light radius of 49.2 of the cluster. According to the simulation by K. Kremer et al. (2021), massive WDs are expected to be found

https://www3.mpifr-bonn.mpg.de/staff/pfreire/GCpsr.html

within the core radius of the cluster. Additionally, a simulation by S. Sigurdsson et al. (1994) demonstrated that blue straggler stars, formed through stellar collisions in the core of the globular cluster M3, may be ejected into the outer regions due to the recoil from these interactions. We speculate that WD 01 may have also been ejected into the outer regions or formed there as a result of similar interactions. The binary system WD 15 is situated far from the core of the cluster, which raises questions about its origin. Therefore, the origin of the binary system WD 15 outside the cluster's core remains uncertain.

The massive WDs found in this cluster could lead to more WD mergers with a possible outcome of neutron star/pulsar formation. In the models of K. Kremer et al. (2021), they assume this will occur if the total mass of the colliding WDs exceeds the Chandrasekhar limit, though it could be slightly more. As young millisecond pulsars have short lifetimes, those formed in the early times are no longer observed at present-day globular clusters. Therefore, currently observed young pulsars are likely formed by merging WDs, WD-MS collisions, along with the recycling of neutron stars through binaries (F. Verbunt & P. C. C. Freire 2014; C. S. Ye et al. 2019). Recently, a massive WD companion to the pulsar PSR J2140-2311B in the corecollapse globular cluster M30 was detected by V. Balakrishnan et al. (2023). With the presence of young massive WDs, NGC 362 is a cluster that may host the progenitors of millisecond pulsars. If the massive WDs of NGC 362 collide, it could lead to the formation of a Type Ia supernova or a neutron star as per Figure 5 of K. Kremer et al. (2023b). If one of the merging WDs has a high magnetic field, this might result in the formation of a

We note that the central core of this cluster is not resolved in the UVIT images, and it may harbor more massive WDs. The cluster is dynamically active with the formation of merged WDs and WD-MS binaries. Therefore, the formation of a magnetar through a WD-WD merger is possible to happen in this globular cluster, and may provide the missing link in the formation pathway of FRB repeaters in a globular cluster in M81 (K. Kremer et al. 2023b). The massive WDs of NGC 362 are, therefore, unique test beds that will provide important inputs to the properties of WDs found in core-collapsed globular clusters.

## 7. Summary and Conclusions

We present a multiwavelength study of 17 WDs in the globular cluster NGC 362 utilizing UVIT/AstroSat and HST data sets. The following conclusions are drawn.

- The UV and UV-optical CMDs were employed to select and classify the WDs. Out of 23 WDs, 17 are found to be isolated.
- 2. Through SED analysis, we determined the fundamental parameters of isolated WDs. The effective temperatures, radii, luminosities, and masses of the WDs are in the ranges 22,000–70,000 K, 0.008–0.028  $R_{\odot}$ , 0.09–3.0  $L_{\odot}$ , and 0.30–1.13  $M_{\odot}$ , respectively.

  3. We find that 14 WDs are single, while three (WD 15,
- 3. We find that 14 WDs are single, while three (WD 15, WD 16, and WD 17) are in binary systems. The binary systems consist of a WD with an M dwarf star. The effective temperatures, radii, luminosities, and masses of M dwarf companions are 3500–3750 K, 0.150–0.234  $R_{\odot}$ , 0.003–0.01  $L_{\odot}$ , and 0.14–0.24  $M_{\odot}$ , respectively.
- 4. The various formation mechanisms of massive WDs and WD-MS binary systems have been discussed. The cooling

age of the WDs implies that they were formed very recently (≤35 Myr). The binary WDs (WD 15, WD 16, and WD 17) and massive WDs (WD 01 and WD 15) may have originated due to the dynamical processes that happened during the core collapse of the cluster. This study provides the first detection of massive WDs in a core-collapsed globular cluster. We suggest that NGC 362 hosts stellar systems that may give rise to neutron stars, Type Ia supernovae, and/or FRBs in the future. Hence, NGC 362 is an ideal test bed to explore the formation pathways of these exotic objects in a globular cluster.

## **ORCID** iDs

```
Arvind K. Dattatrey https://orcid.org/0000-0002-4729-9316
Annapurni Subramaniam https://orcid.org/0000-0003-4612-620X
Geeta Rangwal https://orcid.org/0000-0002-6373-770X
```

### References

Althaus, L. G. 2010, MmSAI, 81, 908

```
Balakrishnan, V., Freire, P. C. C., Ransom, S. M., et al. 2023, ApJL, 942, L35
Bayo, A., Rodrigo, C., Barrado Y Navascués, D., et al. 2008, A&A, 492, 277
Brown, W. R., Kilic, M., Allende Prieto, C., & Kenyon, S. J. 2010, ApJ,
   723, 1072
Calamida, A., Corsi, C. E., Bono, G., et al. 2008, ApJ, 673, L29
Castelli, F., & Kurucz, R. L. 2003, in Modelling of Stellar Atmospheres, ed.
   N. Piskunov, W. W. Weiss, & D. F. Gray, 210 (San Francisco, CA:
Chen, J., Ferraro, F. R., Cadelano, M., et al. 2021, NatAs, 5, 1170
Cheng, S., Cummings, J. D., Ménard, B., & Toonen, S. 2020, ApJ, 891, 160
Cool, A. M., Piotto, G., & King, I. R. 1996, ApJ, 468, 655
Curd, B., Gianninas, A., Bell, K. J., et al. 2017, MNRAS, 468, 239
Dalessandro, E., Ferraro, F. R., Massari, D., et al. 2013, ApJ, 778, 135
Dattatrey, A. K., Yadav, R. K. S., Kumawat, G., et al. 2023a, MNRAS,
   523, L58
Dattatrey, A. K., Yadav, R. K. S., Rani, S., et al. 2023b, ApJ, 943, 130
Elson, R. A. W., Gilmore, G. F., Santiago, B. X., & Casertano, S. 1995, AJ,
Ferraro, F. R., Beccari, G., Dalessandro, E., et al. 2009, Natur, 462, 1028
Hansen, B. M. S., Anderson, J., Brewer, J., et al. 2007, ApJ, 671, 380
Harris, W. E. 2010, arXiv:1012.3224
Hermes, J. J., Kepler, S. O., Castanheira, B. G., et al. 2013, ApJL, 771, L2
Hidalgo, S. L., Pietrinferni, A., Cassisi, S., et al. 2018, ApJ, 856, 125
Ivanova, N., Heinke, C. O., Rasio, F. A., et al. 2006, MNRAS, 372, 1043
Jiménez-Esteban, F. M., Torres, S., Rebassa-Mansergas, A., et al. 2018,
   MNRAS, 480, 4505
Jimenez-Esteban, F. M., Torres, S., Rebassa-Mansergas, A., et al. 2023,
            , 518, 5106
Kepler, S. O., Koester, D., & Ourique, G. 2016, Sci, 352, 67
Kilic, M., Stanek, K. Z., & Pinsonneault, M. H. 2007, ApJ, 671, 761
Kirsten, F., Marcote, B., Nimmo, K., et al. 2022, Natur, 602, 585
Kleinman, S. J., Kepler, S. O., Koester, D., et al. 2013, ApJS, 204, 5
Koester, D. 2010, MmSAI, 81, 921
Kremer, K., Fuller, J., Piro, A. L., & Ransom, S. M. 2023a, MNRAS, 525, L22
Kremer, K., Li, D., Lu, W., Piro, A. L., & Zhang, B. 2023b, ApJ, 944, 6
Kremer, K., Rui, N. Z., Weatherford, N. C., et al. 2021, ApJ, 917, 28
Kremer, K., Ye, C. S., Rui, N. Z., et al. 2020, ApJS, 247, 48
Libralato, M., Bellini, A., van der Marel, R. P., et al. 2018, ApJ, 861, 99
Liebert, J., Bergeron, P., & Holberg, J. B. 2005, yCat, J/ApJS/156/47 Liu, D., Wang, B., Ge, H., Chen, X., & Han, Z. 2019, A&A, 622, A35
Moehler, S., & Bono, G. 2011, arXiv:0806.4456
Napiwotzki, R. & Eso Sn Ia Progenitor Search Consortium 2001, in
   Astronomische Gesellschaft Abstract Series, 18 (Leipzig: AG), MS 09 10
Napiwotzki, R., Karl, C. A., Nelemans, G., et al. 2007, in ASP Conf. Ser. 372,
   15th European Workshop on White Dwarfs, ed. R. Napiwotzki &
   M. R. Burleigh (San Francisco, CA: ASP), 387
Nardiello, D., Libralato, M., Piotto, G., et al. 2018, MNRAS, 481, 3382
```

Petroff, E., Hessels, J. W. T., & Lorimer, D. R. 2019, A&ARv, 27, 4

```
Pichardo Marcano, M., Rivera Sandoval, L. E., Maccarone, T. J., et al. 2025,
   ApJ, 979, 167
Pietrinferni, A., Hidalgo, S., Cassisi, S., et al. 2021, ApJ, 908, 102
Postma, J. E., & Leahy, D. 2017, PASP, 129, 115002
Rebassa-Mansergas, A., Solano, E., Jiménez-Esteban, F. M., et al. 2021,
   MNRAS, 506, 5201
Renzini, A., Bragaglia, A., Ferraro, F. R., et al. 1996, ApJ, 465, L23
Richer, H. B. 1978, ApJL, 224, L9
Richer, H. B., Fahlman, G. G., Ibata, R. A., et al. 1995, ApJL, 451, L17
Richer, H. B., Fahlman, G. G., Ibata, R. A., et al. 1997, ApJ, 484, 741
Rui, N. Z., Kremer, K., Weatherford, N. C., et al. 2021, ApJ, 912, 102
Sigurdsson, S., Davies, M. B., & Bolte, M. 1994, ApJL, 431, L115
Soker, N., Regev, O., Livio, M., & Shara, M. M. 1987, ApJ, 318, 760
Soto, M., Bellini, A., Anderson, J., et al. 2017, AJ, 153, 19
Stetson, P. B. 1987, PASP, 99, 191
Strickler, R. R., Cool, A. M., Anderson, J., et al. 2009, ApJ, 699, 40
```

```
Subramaniam, A., Sindhu, N., Tandon, S. N., et al. 2016, ApJL, 833, L27
Tandon, S. N., Subramaniam, A., Girish, V., et al. 2017, AJ, 154, 128
Temmink, K. D., Toonen, S., Zapartas, E., Justham, S., & Gänsicke, B. T. 2020, A&A, 636, A31
Trager, S. C., King, I. R., & Djorgovski, S. 1995, AJ, 109, 218
Tremblay, P. E., & Bergeron, P. 2009, ApJ, 696, 1755
Vasiliev, E., & Baumgardt, H. 2021, MNRAS, 505, 5978
Verbunt, F., & Freire, P. C. C. 2014, A&A, 561, A11
Vitral, E., Kremer, K., Libralato, M., Mamon, G. A., & Bellini, A. 2022, MNRAS, 514, 806
Weatherford, N. C., Chatterjee, S., Kremer, K., & Rasio, F. A. 2020, ApJ, 898, 162
Wijnen, T. P. G., Zorotovic, M., & Schreiber, M. R. 2015, A&A, 577, A143
Ye, C. S., Kremer, K., Chatterjee, S., Rodriguez, C. L., & Rasio, F. A. 2019,
```

ApJ, 877, 122